Clays and Clay Minerals, Vol. 58, No. 4, 542–557, 2010.

BIOAVAILABILITY OF Fe(III) IN LOESS SEDIMENTS: AN IMPORTANT SOURCE OF ELECTRON ACCEPTORS

MICHAEL E. BISHOP[1], DEB P. JAISI[1,2], HAILIANG DONG[1,3,4,*], RAVI K. KUKKADAPU[5], AND JUNFENG JI[6]

[1] Department of Geology, Miami University, Oxford, OH 45056, USA
[2] Department of Geology and Geophysics, Yale University, PO Box 20820, New Haven, CT 06520, USA
[3] Geomicrobiology Laboratory, State Key Laboratory of Geological Processes and Mineral Resources, China University of Geosciences, Beijing, 100083, China
[4] Key Laboratory of Biogeology and Environmental Geology of Ministry of Education, Faculty of Earth Sciences, China University of Geosciences – Wuhan, Wuhan, 430074, China
[5] Pacific Northwest National Laboratory, Richland, Washington 99352, USA
[6] Department of Earth Sciences, Nanjing University, Nanjing China

Abstract—Fe-reducing micro-organisms can change the oxidation state of structural Fe in clay minerals. The interactions with complex clays and clay minerals in natural materials remain poorly understood, however. The objective of this study was to determine if Fe(III) in loess was available as an electron acceptor and to study subsequent mineralogical changes. The loess samples were collected from St. Louis (Peoria), Missouri, USA, and Huanxia (HX) and Yanchang (YCH), in the Shanxi Province of China. The total Fe concentrations for the three samples was 1.69, 2.76, and 3.29 wt.%, respectively, and Fe(III) content was 0.48, 0.69, and 1.27 wt.%, respectively. All unreduced loess sediments contained Fe (oxyhydr)oxides and phyllosilicates. Bioreduction experiments were performed using *Shewanella putrefaciens* CN32 with lactate as the sole electron donor and Fe(III) in loess as the sole electron acceptor with and without anthraquinone-2, 6-disulfonate (AQDS) as an electron shuttle. Experiments were performed in non-growth (bicarbonate buffer) and growth (M1) media. The unreduced and bioreduced solids were analyzed by X-ray diffraction, Mössbauer spectroscopy, diffuse reflectance spectroscopy, and scanning electron microscopy/energy dispersive spectroscopy. Despite many similarities among the three loess samples, the extent and rate of Fe(III) reduction varied significantly. In the presence of AQDS the extent of reduction in the non-growth experiment was 25% of total Fe(III) in HX, 34% in Peoria, and 38% in YCH. The extent of reduction in the growth experiment was 72% in HX, 94% in Peoria, and 65% in YCH. The extent of bioreduction was less in the absence of AQDS. Overall, AQDS and the M1 growth medium significantly enhanced the rate and extent of bioreduction. Fe(III) in (oxyhydr)oxides and phyllosilicates was bioreduced. Siderite was absent in control samples, but was identified in bioreduced samples. The present research suggests that Fe(III) in loess sediments is an important potential source of electron acceptors that could support microbial activity under favorable conditions.

Key Words—Bioreduction, Iron, Loess, Mineral Transformation, *Shewanella putrefaciens*.

INTRODUCTION

Clays and clay minerals are important components in soils, sediments, and sedimentary rocks, and play important roles in many environmental processes such as nutrient cycling, plant growth, and contaminant migration (Stucki *et al.*, 2002; Stucki and Kostka, 2006; Dong *et al.*, 2009). Many clay minerals contain structural Fe, and the redox state of the Fe determines the physical and chemical properties of these fine-grained minerals, which in turn affect many environmental processes (Stucki, 2006; Dong *et al.*, 2009). Past research has shown that Fe-reducing micro-organisms can change the oxidation state of structural Fe in pure clay minerals (Gates *et al.*, 1998; Kostka *et al.*, 1999a, 1999b; Dong *et al.*, 2003a, 2003b; Shelobolina *et al.*, 2003; Kim *et al.*, 2004; Jaisi *et al.*, 2005; Stucki, 2006). However, little attention has been paid to the interactions of micro-organisms with complex clays and clay minerals present in natural materials. One such material is found in clay-rich loess deposits.

Loess is an eolian sedimentary deposit that consists of various clay- and silt-sized minerals. Loess and loess-like sediments cover as much as 10% of the Earth's surface, and form some of the world's most productive soils (Smalley, 1975; Smalley *et al.*, 2001). Distribution of loess is restricted to areas such as arid and semi-arid climatic zones and former periglacial regions (Dolgoff, 1998). Iron (oxyhydr)oxides and clay minerals are commonly found in natural loess deposits in China and the United States (Muhs and Bettis; 2000; Muhs and Zarata; 2001; Gallet *et al.*, 1996; Jahn *et al.*, 2001) and these minerals typically contain structural Fe(III).

Iron (oxyhydr)oxides and clay minerals co-exist with micro-organisms in loess deposits and, as a result, these fine-grained minerals may undergo biotic reactions.

* E-mail address of corresponding author:
dongh@muohio.edu
DOI: 10.1346/CCMN.2010.0580409

Chen *et al.* (2003) studied formation mechanisms of magnetic minerals in loess samples from China and observed that magnetite and maghemite are major magnetic minerals in loess-paleosol sequences. Chen *et al.* (2003) inferred that only a fraction of the magnetite and maghemite formed by the pedogenic weathering of chlorite and that the presence of small amounts of phosphorous (P) and sulfur (S) suggest a biogenic origin. Chen *et al.* (2005) further examined maghemite and magnetite in Chinese loess samples and concluded that nanocrystalline maghemites with nanoporous textures resulted from microbe-induced precipitation of magnetite or by transformation of poorly crystalline Fe(III) (oxyhydr)oxides in the presence of Fe-reducing bacteria. Those authors proposed that aggregates of euhedral maghemite nanocrystals were transformed from magnetite magnetosomes that are typically produced by magnetotactic bacteria (Bazinlynsky and Frankel, 2004). Indeed, Jia *et al.* (1996) isolated magnetotactic bacteria in the Duanjiapo loess sections in China. More recently, Xu and Chen (2008) presented evidence for microbe-templated calcite nano-fibers in Chinese loess samples, which suggest microbial activity in loess deposits. All of these studies suggest that loess deposits, although frequently dry, may host microbial communities. Microbial communities may be important to biogeochemical processes either over a long time scale or during initial weathering and episodic precipitation events.

The presence of microbial communities in dry environments is common (Chanal *et al.*, 2006; Dong *et al.*, 2007; Osman *et al.*, 2008). The formation of distinct mineralogical deposits in deserts (known as desert varnish) has been associated with microbial activity (Dorn and Oberlander, 1981; Perry *et al.*, 2003). Iron/manganese oxide deposits and clay particles in desert varnish from the western United States were found to be associated with *metallogenium*- and *Pedomicrobium*-like bacteria (Dorn and Oberlander, 1981). In conclusion, little water, high temperatures, and the lack of abundant organic matter in deserts (Dorn and Oberlander, 1981) do not exclude microbial activity. Some micro-organisms, such as *Shewanella*, *Geobacter*, and other dissimilatory metal-reducing bacteria (DMRB), have been found to exist in extreme environments (Lovely, 1991; Wang *et al.*, 2004). Very little is known about the role of such micro-organisms in naturally occurring loess deposits, however.

The focus of this research was to determine if Fe(III) in loess was available as an electron acceptor to support microbial life, and to investigate changes in mineralogy due to bacterial utilization of Fe(III). In order to achieve this goal, three different desert loess sediment samples were collected on two continents. The samples were then subjected to microbial Fe(III) reduction in non-growth and growth media. The extent and rate of bioreduction were determined by wet chemistry methods, and mineralogical changes were characterized by X-ray diffraction (XRD), scanning electron microscopy (SEM) with energy dispersive spectroscopy (EDS), Mössbauer spectroscopy, and diffuse reflectance spectroscopy (DRS).

MATERIALS AND METHODS

Loess collection and preparation

Three representative loess samples, one from the USA and two from China, were chosen for this study.

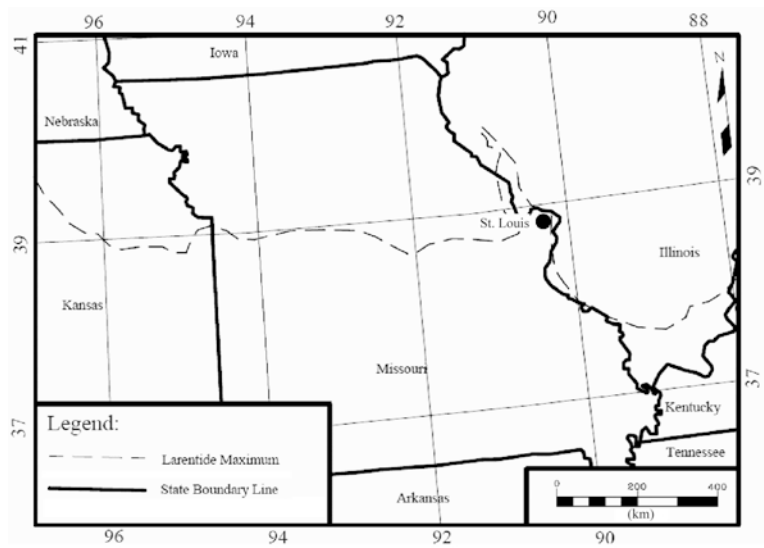

Figure 1. Sketch map of Missouri showing the Larentide Ice Sheet at its maximum. The solid circle showing St. Louis, Missouri, is the location for the Peoria Loess sample used in this study.

https://doi.org/10.1346/CCMN.2010.0580409 Published online by Cambridge University Press

The USA loess sample, kindly provided by Dr Jason Rech (Miami University, Oxford, Ohio), was collected from a site near St. Louis, Missouri, USA (Figure 1). The loess site is located along the east bank of the Mississippi River Valley on the eastern boundary of Missouri and the southwestern boundary of Illinois, ~120 km southwest of the maximum advance of the Laurentide ice sheet during the late Wisconsin epoch (Wang *et al*., 2003). The USA loess sample is from the Peoria Loess Belt, which in USGS maps spans the general area 1500 km east–west from Colorado to Illinois and 1500 km north–south from Wisconsin to southern Illinois (Thorp and Smith, (1952). The loess sample used in this study is the most widely distributed loess unit in the USA with thicknesses up to 50 m in southwestern Nebraska (Maat and Johnson, 1996; Roberts *et al.*, 2003) and is overlain by a Late Wisconsin Peoria Loess unit. The Peoria loess sample (~10,000–27,000 B.P.) used in this study was collected beneath a late Wisconsin Peoria Loess unit and just above the underlying Roxanna Silt (~27,000–55,000 B.P.) (Leigh, 1994; Grimley *et al.*, 1998; Grimley, 2000; Muhs and Bettis, 2000; Wang *et al.*, 2000, 2003).

The China loess samples were collected from two different sites in the central part of the Loess Plateau in north central China. The Huanxian (36º37′N, 107º19′E) (HX) section is situated in the sandy loess transition zone of the Loess Plateau (Figure 2). The section is ~23 m thick and located in the semi-arid temperate zone with a mean annual temperature and precipitation of 7.6ºC and 400 mm, respectively. The Yanchang (36º60′N, 110º02′E) (YCH) section is located on the central part of the Loess Plateau, ~180 km east of the Huanxian section (Figure 2). This section is ~19 m thick and located in the semi-humid temperate zone with mean annual temperature and precipitation of 10.4ºC and 596 mm, respectively (Ji *et al.*, 2004).

The Peoria, Huanxian, and Yanchang loess deposits are famous worldwide and the paleoclimatic implications of these deposits have been examined (Grimley *et al.*, 1998; Grimley, 2000; Muhs and Bettis, 2000; Wang *et al.*, 2000, 2003; Sun, 2002; Hu *et al.*, 2004). Each loess sample was soaked thoroughly in water and ground sufficiently to disperse loess aggregates, but not enough to break primary mineral grains. The ground loess samples were dried in an oven for 24 h at 60ºC. Stock solutions were prepared with 100 mg/mL of loess in a filter-sterilized bicarbonate buffer, purged with N_2:CO_2 (80:20) to remove dissolved oxygen, and then autoclaved.

Bacterial culture

Shewanella putrefaciens strain CN32 cells were routinely cultured aerobically in tryptic soy broth (TSB) from frozen stock culture, which was kept in 35% glycerol at −80ºC. After harvesting in TSB until the mid- to late-log phase, CN32 cells were washed three times in filter-sterilized bicarbonate buffer (2.5 g/L of reagent-grade $NaHCO_3$ and 0.1 g/L of KCl) by repeated centrifugation and resuspension. Final CN32 cell suspensions were prepared in a sterile bicarbonate buffer, and cell concentrations were measured in colony forming units (CFU).

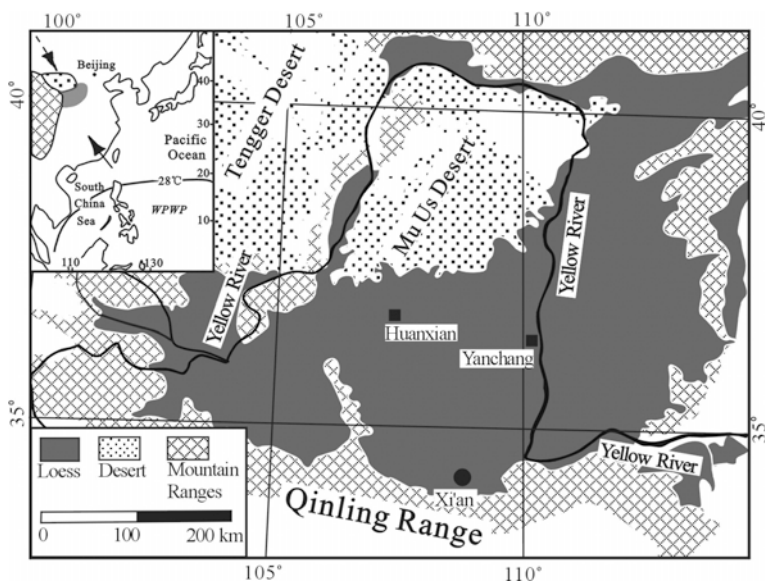

Figure 2. Sketch map of the Loess Plateau of China, showing the location of the HX and YCH loess-paleosol sections used in the present study, in relation to Xi'an and the Yellow River. The inset shows the geographic location of the Loess Plateau relative to the Pacific Ocean and to Beijing. The arrow indicates the SE limit of the Loess Plateau. The figure is adapted from Ji *et al.* (2002)

https://doi.org/10.1346/CCMN.2010.0580409 Published online by Cambridge University Press

Bioreduction experiments

Two different Fe-reduction experiments were performed for each loess sample: a non-growth medium was used for the first experiment and a growth medium for the second. The non-growth experiment was performed with Fe(III) in autoclaved loess sediment (20 mg/mL final concentration) as the sole electron acceptor and filter-sterilized lactate (20 mM final concentration) as the sole electron donor in a filter-sterilized bicarbonate buffer with a final cell concentration of $\sim 5.5 \times 10^8$ cells/mL. In selected tubes, filter-sterilized anthraquinone-2, 6-disulfonate (AQDS) with a final 0.1 mM concentration was added to act as an electron shuttle to facilitate electron transfer from lactate to Fe(III) in the loess samples. The AQDS was used as an analog to humic acids from natural environments. The control tubes contained an equivalent volume of bicarbonate buffer instead of CN32 cells. The growth experiment consisted of defined M1 growth medium (Myers and Nealson, 1988) in place of bicarbonate buffer. The M1 medium contained 20 mM lactate as the electron donor in a base medium of the following composition (in 1 L of H_2O): 9.0 mM $(NH_4)_2SO_4$, 5.7 mM K_2HPO_4, 3.3 mM KH_2PO_4, 5.4 μM $FeSO_4 \cdot 7H_2O$, 67.2 μM Na_2EDTA, 0.485 mM $CaC1_2 \cdot 2H_2O$, 1.01 mM $MgSO_4 \cdot 7H_2O$, 56.6 μM H_3BO_3, 3.87 μM $Na_2MoO_4 \cdot 2H_2O$, 1.26 μM $MnSO_4 \cdot H_2O$, and 1.04 μM $ZnSO_4 \cdot 7H_2O$. The solution was homogenized followed by addition of 1.5 μM Na_2SeO_4, 10.0 μM NaC1, 5.0 μM $CoSO_4$, and 5.0 μM $Ni(NH_4)_2(SO_4)_2 \cdot 6H_2O$. The solution was purged with 80:20 N_2:CO_2 for 20 min for aqueous solution and 20 min for headspace. The solution was then autoclaved for 30 min followed by addition of filter-sterilized 2.0 mM $NaHCO_3$ to make 1 L total volume. The pH was adjusted to 7.0 with 1 M NaOH solution. The final cell concentration in the growth experiment was $\sim 2.1 \times 10^6$ cells/mL. Other conditions for the growth experiment were identical to those used for the non-growth experiment.

All experimental ingredients including media, AQDS in select tubes, lactate, and loess stock suspensions were added to autoclaved 25 mL Balsch tubes in a sterile workbench. The tubes were purged with N_2:CO_2 gas mix (80:20) for 20 min and sealed with thick butyl rubber stoppers. The CN32 cells were added to the tubes with a 1-cc syringe, which had been purged 15 times with N_2:CO_2 gas mix (80:20) prior to use. The tubes were then incubated at 37ºC with shaking at 60 rpm. All treatments and measurements were carried out under strictly sterile and anoxic conditions. All experiments were run in duplicate and an average was obtained for time-course Fe(II) concentration measurements.

Analytical methods

Measurement of total Fe and Fe(II) concentration by direct current plasma emission spectrometry (DCP) and titration, respectively. The unreduced loess samples were ground and heated to 100ºC overnight to ensure that the samples were completely dry. For total Fe content measurement, 300 mg of lithium metaborate ($LiBO_2$) flux was added to a 100 mg sample. The flux-sample mixture was fused at 995ºC in a graphite crucible for 10 min. The molten mixture was added to 100 g of HNO_3, placed on a shaker table overnight, and analyzed by DCP for total Fe content. A fraction of the three loess samples was titrated using the Andrade *et al.* (2002) method to determine Fe(II) concentration. The Fe(III) concentration was determined by the difference between the total and Fe(II) concentration.

Ferrozine and 1,10-phenanthroline analysis for Fe(II). At selected time points over the course of the bioreduction experiments, the culture tubes were removed from the incubator and 0.5 mL of cell-mineral suspension was sampled with a sterile and anoxic syringe and was added to the bottom of a 1.5 mL Eppendorf tube containing 0.5 mL of 1 N Ultrex HCl. The acid extraction was allowed to digest for 24 h prior to Fe(II) measurements. The Fe(II) concentration in the extract was determined by the Ferrozine assay (Stookey, 1970). Because of the presence of sands and silts in the loess samples, sampling with a syringe may have introduced sampling bias, *i.e.* fine-grained oxides and phyllosilicates may have been sampled preferentially. Assuming that these minerals had greater overall Fe contents and were more reducible, the biased sampling would overestimate the extents of bioreduction. Therefore, the reported extents of bioreduction may represent maximum values. Because all the unreduced samples contained an initial amount of Fe(II), this amount was, therefore, subtracted from the Fe(II) concentration measured when the extent of bioreduction was calculated at each time point.

Concentrations of Fe(II) in the bioreduced samples from the non-growth experiments were also determined using the 1,10 phenanthroline method (Amonette and Templeton, 1998) because previous studies have shown that 0.5 N HCl extraction underestimates total biogenic Fe(II) in silicates, such as nontronite (Jaisi *et al.*, 2007; Anastácio *et al.*, 2008), and XRD analysis identified phyllosilicates in the loess samples. Only an initial and final Fe(II) analysis by the 1,10 phenanthroline method was performed. This method was not used for Fe(II) analysis from the growth experiment because of lack of a sufficient amount of bioreduced sample. For this reason, the extent of bioreduction was calculated based on the Ferrozine assay, and probably represented an underestimate.

The bioreduced non-growth experiment samples were analyzed for aqueous concentrations of the major and trace elements P, Mg, Si, Mn, Fe, Ti, Al, Ca, K, and Na by DCP to measure possible loess dissolution after filtration of the samples through a 0.22 μm filter and the addition of an equal volume of 1 N HCl (1:1 ratio). The amount of suspension volume was insufficient to measure aqueous elemental concentrations for the growth-experiment bioreduced samples.

https://doi.org/10.1346/CCMN.2010.0580409 Published online by Cambridge University Press

Cell counting. At selected time points over the course of the bioreduction experiments, aliquots of loess-cell suspension were spread onto TSB agar plates and CFU were numerated after 24 h of aerobic incubation.

Mineralogical analyses

X-ray diffraction. Smear mounts (Moore and Reynolds, 1997) were prepared for the unreduced and bioreduced loess samples and X-ray diffraction (XRD) scans were collected and examined to determine the mineralogy. The bioreduced samples were prepared and kept inside the glove box until analysis. Powder XRD patterns were collected using a Scintag XDS-2000 diffractometer using CuKα radiation, a fixed slit scintillation detector, and 1400 W of power (40 kV, 35 mA) (Scintag, Inc., Cupertino, California). Following XRD analyses, the same slides were subsequently solvated with ethylene glycol (EG) in a desiccator at room temperature for 24 h to expand the smectite interlayers. The XRD patterns were obtained immediately after EG saturation without significant exposure to air in a humidity-controlled laboratory. Qualitative identification of mineral phases was determined using the *Jade 7* program, which utilizes the International Center for Diffraction Data Powder Diffraction File database (ICDD PDF-2, Sets 1-46, 1996) as the reference source.

Diffuse reflectance spectroscopy (DRS). Both unreduced and bioreduced samples were analyzed by DRS in order to estimate hematite and goethite concentrations using the method described by Ji *et al.* (2002). Reflectance spectra of the samples were obtained using a Perkin-Elmer Lambda 6 spectrophotometer with a diffuse reflectance attachment from 250 to 850 nm. Ground samples (100 mg) were made into a slurry on a glass microslide with distilled water, smoothed, and dried slowly at low temperature (<40ºC). Reflectance data were processed to obtain percent reflectance in standard color bands (Judd and Wyszecki, 1975). Percent reflectance in the standard color bands was calculated by dividing the percentage of reflectance in a color band by the total reflectance in a sample. The total reflectance or brightness of a sample (Balsam and Li, 1999) was calculated by summing a sample's reflectance values from 400 to 700 nm.

Mössbauer spectroscopy. Mössbauer spectra were collected at room temperature (RT), 77 K, and 4.5 K to examine Fe mineralogy of the YCH control and bioreduced loess sample in a growth medium containing AQDS. Randomly oriented absorber disks were prepared by mixing ~100 mg of dried loess sample with petroleum jelly. The disks were stored at −80ºC in an anoxic chamber until analysis. Details of absorber preparation and instrumentation were identical to those reported by Kukkadapu *et al.* (2004). The data were modeled with recoil software (University of Ottawa, Canada) using the Voigt-based spectral fitting routine (Rancourt and Ping, 1991).

Scanning electron microscopy and energy dispersive spectroscopy (SEM/EDS). The unreduced and bioreduced samples were mounted on Poly-L-Lysine-treated 15-mm round glass cover slips followed by ethanol (ETOH) dehydration. The samples were critical point dried with a Tousimis Samdri-780A Critical Point Dryer, and then carbon coated (20 nm) with an Anatec, Ltd., Hummer VI Sputter Coater. The samples were analyzed using a Zeiss Supra 35 VP SEM with EDAX Genesis 2000 X-ray energy dispersive spectroscopy (SEM/EDS). The EDS chemical spectral data served as the primary means of qualitative mineral identification.

Grain-size analysis. 2 g of each loess sample was sieved utilizing a US standard mesh size No. 230 (0.0625 mm square), the material retained on the sieve was considered to be sand size and weighed ($sand_{wt}$). The material that passed through the No. 230 sieve was suspended in water for a few minutes, centrifuged at $100 \times g$ for 6 min, and the resulting silt fraction was dried at 60ºC overnight and weighed ($silt_{wt}$). The supernatant was then centrifuged at $8000 \times g$ for 48.23 min to obtain the clay fraction ($clay_{wt}$). The sum of the three size fractions was compared to the starting weight to determine the % error

$$\% \text{ error} = \text{ABS}((\text{sand}_{wt} + \text{clay}_{wt} + \text{silt}_{wt}) - \text{sample}_{wt})/\text{sample}_{wt} \times 100$$

RESULTS

Characterization of the unreduced loess sediments

Grain size and Fe concentration. The Peoria loess sample had a grain size of 10% sand, 88% silt, and 2% clay (Table 1). Both China loess samples (HX and YCH) had the same grain-size distribution, *i.e.* 72% sand, 26% silt, and 2% clay (Table 1). The total Fe contents of the Peoria, HX, and YCH loess samples were 1.69, 2.76, and 3.29 wt.%, respectively, and the Fe(III) contents were 0.48%, 0.69%, and 1.27%, respectively (Table 1). These Fe(III) contents corresponded to an Fe(III) working concentration in the bioreduction tubes of 46 μM, 24 μM, and 17 μM for the Peoria, HX, and YCH samples, respectively.

Table 1. Soil textural classification of loess samples with Fe content (%).

Soil type:	HX loess Sandy loam	Peoria loess Silt loam	YCh loess Sandy loam
Sand	72%	10%	72%
Silt	26%	88%	26%
Clay	2%	2%	2%
% Error	1%	0%	0%
Total Fe	2.76%	1.69%	3.29%
Total Fe(III)	0.69%	0.48%	1.27%

https://doi.org/10.1346/CCMN.2010.0580409 Published online by Cambridge University Press

Mineralogy. The XRD patterns indicated that the three unreduced loess sediments had similar compositions with major minerals quartz, feldspars, calcite, and dolomite (Table 2 and Figure 3). The dominant clay minerals were illite, smectite, chlorite, and kaolinite. Minor amounts of hematite, maghemite, and goethite were detected in the Peoria and HX loess samples, but only minor goethite was detected in the YCH loess. The DRS scans were generally consistent with the XRD data in detecting the presence or absence of Fe (oxyhydr)-oxides (Figure 4).

The SEM observations of the loess samples showed that the average grain size was generally <0.15 mm. Some particles with platy morphology observed at high magnification were confirmed as phyllosilicates using EDS chemical data. The EDS spectra of all three loess samples displayed some Fe, Ti, and Zn peaks in phyllosilicates. Some Fe and Fe/Ti oxides were detected in the three samples with a combination of back-scattered electron (BSE) imaging and EDS.

In the pristine YCH loess sample, ~40% of the total Fe existed as Fe(II) in clay minerals (Figure 5a–c), in good agreement with the wet-chemistry data (Table 1). A fraction of the Fe(II) exhibited magnetic order at 4.5 K (Figure 5). The distribution of Fe(II) in different environments was readily evident from a comparison of the 4.5 K spectrum with that obtained above 77 K. Only a single Fe(II) doublet was present in the RT and 77 K spectra, but two Fe(II) doublets were apparent at 4.5 K [clay Fe(II)-1 and clay Fe(II)-2]. The Fe(II)-rich clays (*e.g.* chlorite) partially ordered magnetically at 4.5 K, and the spectral features of the clay Fe(II)-2 at 4.5 K were similar to those noted in a Mediterranean sediment containing Fe-rich clays (Van Der Zee *et al.*, 2005). The data implied the presence of Fe(II) in both Fe-poor and Fe-rich clays, in agreement with the

Table 2. Mineralogy of the HX, Peoria, and YCH loess sediments in both bicarbonate buffer and M1 growth media determined by XRD.

	Control			Without AQDS			With AQDS		
	HX	Peoria	YCH	HX	Peoria	YCH	HX	Peoria	YCH
Non-growth media									
Albite	x	–	–	x	–	–	x	–	–
Anorthite	x	x	x	x	x	x	x	x	x
Calcite	x	–	x	x	–	x	x	–	x
Jarosite	–	x	–	–	x	–	–	x	–
Quartz	x	x	x	x	x	x	x	x	x
Siderite	–	–	–	–	–	–	–	–	x
Vivianite	x	x	–	x	x	–	x	x	–
Zeolite	x	–	–	x	–	–	x	–	–
Chlorite	x	x	x	x	x	x	x	x	x
Illite	x	x	x	x	x	x	x	x	x
Kaolinite	x	x	x	x	x	x	x	x	x
Smectite	x	–	x	x	–	x	x	–	x
Goethite	x	x	–	x	x	–	x	x	–
Hematite	x	x	–	x	x	–	x	–	–
Maghemite	x	–	x	x	–	x	x	–	x
M1 growth media									
Albite	x	–	–	x	–	–	x	–	–
Anorthite	x	x	x	x	x	x	x	x	x
Calcite	x	–	x	x	–	–	x	–	–
Jarosite	–	x	–	–	–	–	–	–	–
Quartz	x	x	x	x	x	x	x	x	x
Siderite	–	–	–	x	–	x	x	–	x
Vivianite	x	x	–	x	x	–	x	x	–
Zeolite	x	–	–	x	–	–	x	–	–
Chlorite	x	x	x	x	x	x	x	x	x
Illite	x	x	x	x	x	x	x	x	x
Kaolinite	x	x	x	x	x	x	x	x	x
Smectite	x	–	x	x	–	x	x	–	x
Goethite	x	x	–	x	–	–	x	–	–
Hematite	x	x	–	x	–	–	x	–	–
Maghemite	x	–	x	x	–	–	x	–	–

Control: loess + lactate + medium
without AQDS: loess + lactate + medium + cells
with AQDS: loess + lactate + medium + cells + AQDS

https://doi.org/10.1346/CCMN.2010.0580409 Published online by Cambridge University Press

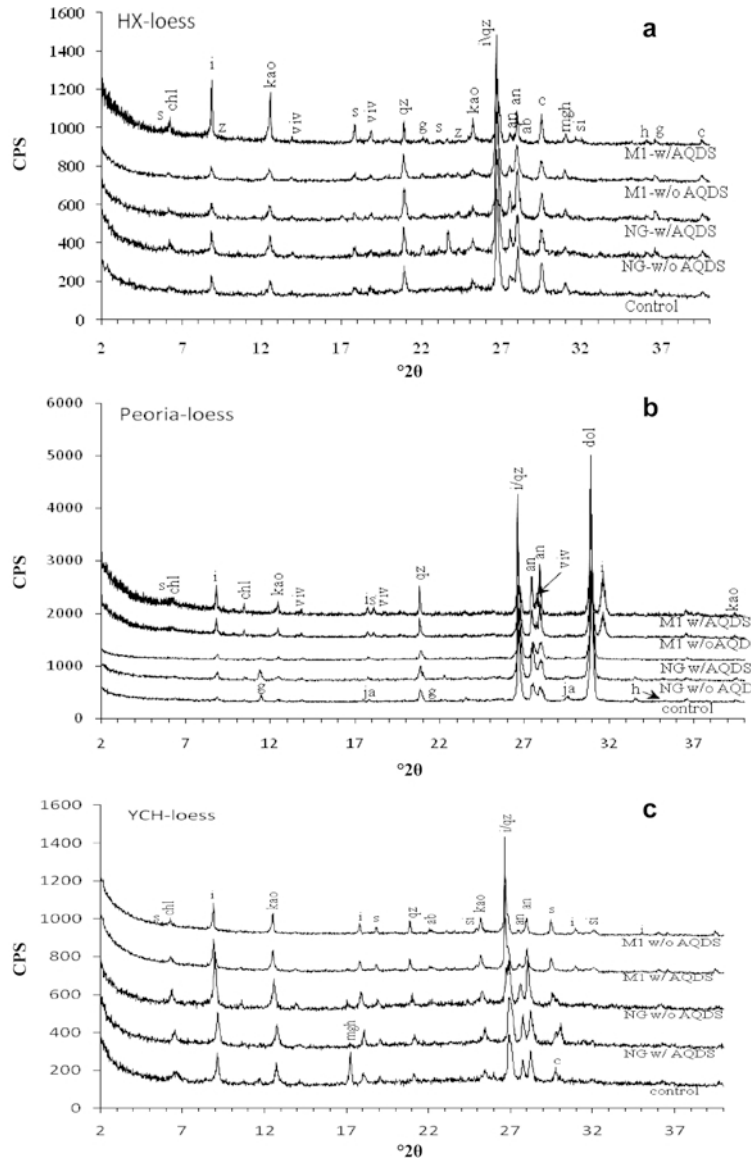

Figure 3. XRD patterns of unreduced and bioreduced loess sediments for (a) the HX loess sample, (b) the Peoria loess sample, and (c) the YCH loess sample. Miscellaneous minerals (ab – albite; an – anorthite; c – calcite; dol – dolomite; ja – jarosite; qz – quartz; si – siderite; viv – vivianite; z – zeolite). Phyllosilicates (chl – chlorite; i – illite; kao – kaolinite; s – smectite). Fe (oxyhydr)oxides (g – goethite; h – hematite; mgh – maghemite).

presence of various clay minerals in this sample (Table 2). Only a small fraction, ~5%, of the Fe(III) was crystalline hematite, consistent with the DRS data (Figure 4). The nature of the remaining Fe(III) was rather complex, and was a mix of Fe(III) (oxyhydr)-oxides that were small-particle (SP) and/or substituted (SO) (*e.g.* Al-goethite), and clay Fe(III). The SP and SO peaks existed as doublets above 77 K but were resolved/partially ordered (PO) at 4.5 K. The SP and SO fractions suggest the presence of goethite, again consistent with the DRS data. The Mössbauer-derived average Fe(II)/Fe(III) ratio for clay minerals was ~1, based on the fit-derived clay Fe contents of the 4.5 K spectrum (Table 3; clay Fe(III) was 42%; clay Fe(II)-1 + clay Fe(II)-2 was 38%).

Microbial reduction of Fe(III) in the loess samples

The *S. putrefaciens* CN32 strain used Fe(III) in the loess samples as the sole electron acceptor for lactate oxidation. In general, bioreduction of Fe(III) in the non-growth experiments was less than in the growth experiments. Relative to the treatment without AQDS, treatment with AQDS greatly stimulated Fe(III) reduction, which was indicated by a rapid increase in HCl-

https://doi.org/10.1346/CCMN.2010.0580409 Published online by Cambridge University Press

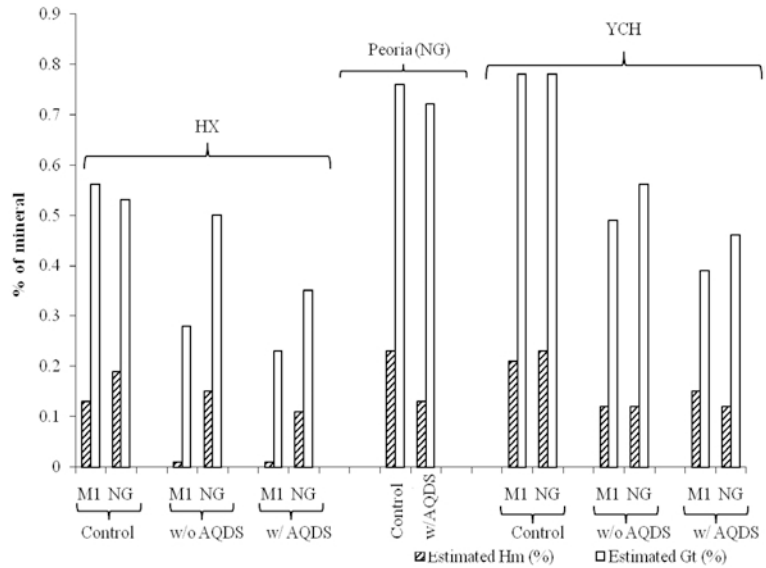

Figure 4. DRS estimate of goethite and hematite contents in unreduced and bioreduced loess samples. HX shows a decrease in hematite and goethite; Peoria shows a reduction in both hematite and goethite; and YCH shows a decrease in hematite and goethite after bioreduction (w/o: without; w: with; HM; hematite; Gt: goethite).

extractable Fe(II) with time (Figure 6). In the non-growth experiment, the extent of bioreduction for the three samples ranged from 17–28% without AQDS to 25–38% with AQDS based on the initial Fe(III) contents and the assumption that HCl-extractable Fe(II) increases were due to Fe(III) bio-reduction (Figures 6, 7). The HX sample had the least bio-reduction and the YCH sample the greatest. The extents of bio-reduction based on the 1,10-phenanthroline Fe(II) contents were consistently 1.14–1.18 times greater than HCl-extractable Fe(II) contents for all three loess samples in the non-growth medium (Figure 6).

The extents of bioreduction for the growth experiments as measured by 0.5 N HCl extractions, *i.e.* 52–53% without AQDS and 65–94% with AQDS, were much greater than those for the non-growth experiments as measured by the same method (Figures 6, 7). In the growth experiment, the YCH loess sample had the least bio-reduction and the Peoria sample the greatest at 94%, with minimal bio-reduction in the growth and non-growth control experiments (Figures 6, 7).

The bioreduced, non-growth medium, HX sample without AQDS had increased aqueous Fe and Mn concentrations relative to the abiotic control (Table 3). Bioreduction of the Peoria sample released Si, Mg, and Al into aqueous solution (Table 3). The aqueous concentrations of major and minor elements in the bioreduced YCH sample were similar to those in the abiotic control (Table 3).

The CFU in the non-growth experiment decreased from ~5.5×10^8 at the beginning of the bioreduction to ~2.6×10^8 cells/mL at the end (Figure 8). In contrast, the CFUs in growth experiments increased from ~2.1×10^6 at the start to ~4.1×10^8 cells/mL at the end of the experiments.

Table 3. Aqueous concentrations of selected elements (mM) for the abiotic control (*C*) and the biotic treatment without (w/o) AQDS in the non-growth experiment, as determined by DCP spectroscopy.

	HX		Peoria		YCH	
	C	w/o	*C*	w/o	*C*	w/o
P	0.24	0.21	0.21	0.21	0.03	0.02
Mg	1.72	1.46	1.47	1.76	0.21	0.17
Si	1.98	1.98	1.29	2.18	0.34	0.24
Mn	0.01	0.01	0.01	0.02	0.00	0.01
Fe	0.09	0.20	0.23	0.19	0.08	0.04
Al	0.00	0.04	0.01	0.04	0.00	0.00
Ca	0.48	0.27	0.51	0.29	1.13	1.15
K	0.00	0.00	0.00	0.00	0.71	0.73
Na	0.14	0.08	0.16	0.008	0.50	0.50

https://doi.org/10.1346/CCMN.2010.0580409 Published online by Cambridge University Press

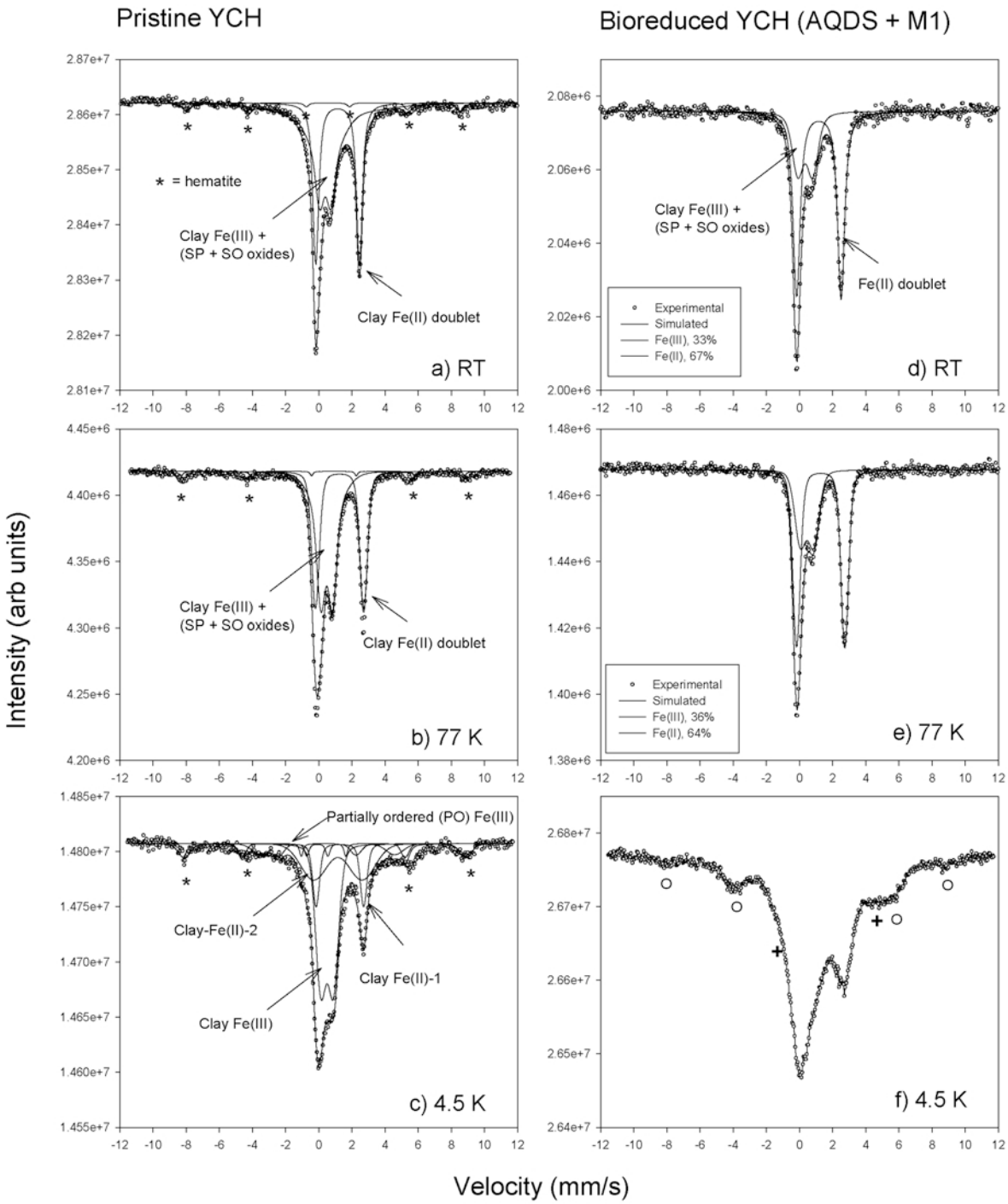

Figure 5. Variable-temperature Mössbauer spectra of pristine YCH and bioreduced YCH (AQDS + M1). * = hematite sextet; SP = superparamagnetic; SO = substituted (oxyhydr)oxide (*e.g.* Al-goethite); in the pristine sample, clay Fe(II) is split into two doublets at 4.5 K (low- and high-Fe(II) containing clays). The 4.5 K bioreduced spectrum was not modeled because of complexity (o: residual SP and SO Fe (oxyhydr)oxide).

Mineralogical changes as a result of bioreduction

In all of the loess samples, goethite and hematite (and perhaps some maghemite) were the main minerals bioreduced (Table 4). In general, goethite and hematite (maghemite) XRD peaks were present in the abiotic control, but these peaks either disappeared or were of lesser intensity after bioreduction (Figure 3). The DRS spectra indicated similar results (Figure 4), *e.g* a

https://doi.org/10.1346/CCMN.2010.0580409 Published online by Cambridge University Press

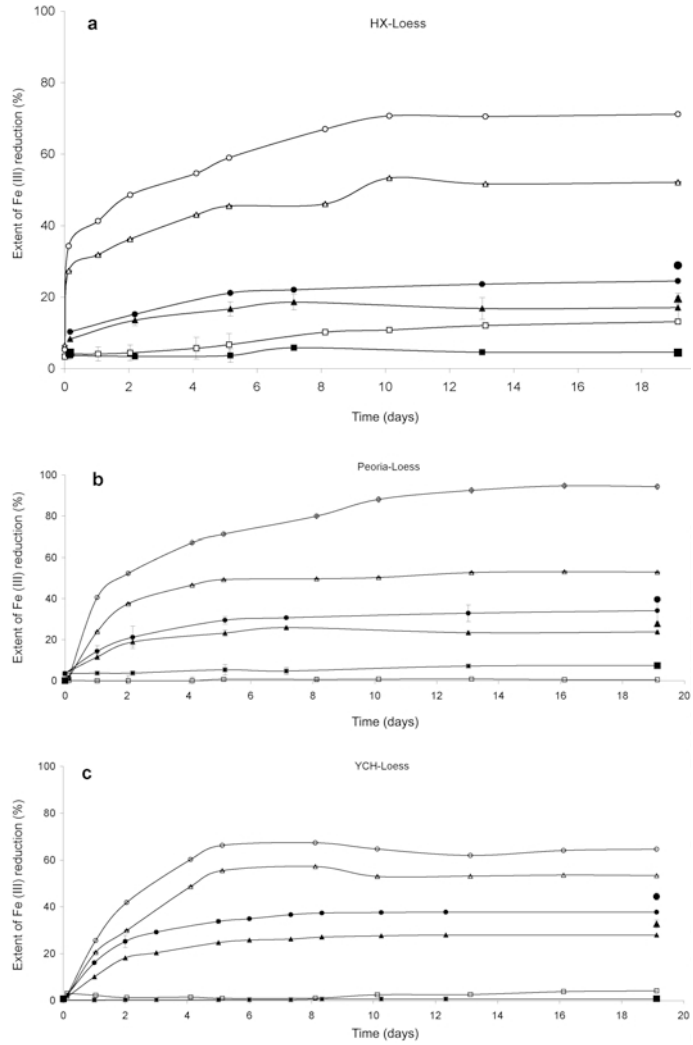

Figure 6. HCl-extractable Fe(II) concentration with time in non-growth and growth experiments. At the end of the bioreduction experiments (last time point), the 1,10 phenanthroline method was used to measure total Fe(II); (a) HX; (b) Peoria; (c) YCH. Note: The large, filled square, filled circle, and filled triangles are for 1,10 Phenanthroline measurements (non-growth experiment). ■: Loess + lactate + bicarb. buffer; ▲: loess + lactate + bicarb. buffer + CN32 cells; ●: loess + lactate + bicarb. buffer + CN32 cells + AQDS; –■–: loess + lactate + bicarb. buffer; –▲–: loess + lactate + bicarb. buffer + CN32 cells; –●–: loess + lactate + bicarb. buffer + CN32 cells + AQDS; –□–: loess + lactate + M1 medium; –△–: loess + lactate + M1 medium + CN32 cells; –○–: loess + lactate + M1 medium + CN32 + AQDS.

decrease in goethite and hematite contents was observed in the non-growth-medium HX sample after bioreduction (Figure 4). The DRS spectra for the M1 medium HX sample indicated nearly complete hematite reduction and partial goethite reduction. The non-growth-medium Peoria sample DRS spectra suggest that bioreduction partially decreased the goethite and hematite contents. Goethite was only detected in the unreduced YCH sample by XRD, but the lower detection limit of DRS allowed identification of both goethite and hematite. A decrease in goethite and hematite contents after bioreduction treatments suggests these (oxyhydr)oxides were reduced in the YCH sample.

In addition to reduction of Fe (oxyhydr)oxides, certain phyllosilicates were also biologically reduced. For example, the aqueous Si and Al concentrations of the non-growth medium Peoria sample increased from 1.29 to 2.18 mM and from 0.01 to 0.04 mM, respectively, after bioreduction (Table 3). The nearly complete reduction of the Peoria sample demonstrated that Fe(III) in phyllosilicates was bioreduced, as phyllosilicates were the dominant Fe(III)-containing minerals in this sample.

Further reduction of Fe (oxyhydr)oxides and phyllosilicates was evident from the Mössbauer data. A decreased area of the 77 K Mössbauer spectra sextet (Figure 5d–e) for the bioreduced YCH loess sample in

https://doi.org/10.1346/CCMN.2010.0580409 Published online by Cambridge University Press

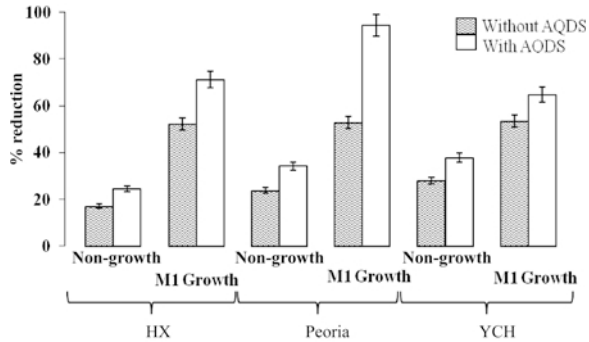

Figure 7. A summary bar graph comparing the extents of bioreduction, with and without AQDS, in non-growth and in the M1 growth experiments for the three loess samples.

M1 medium with AQDS suggests that Fe(III) in goethite and hematite was partially reduced and this is consistent with the XRD and DRS data. The central Fe(III) doublet area decreased in intensity relative to the abiotic control (Figure 5), suggesting partial reductive dissolution of the SP/SO (oxyhydr)oxides (in agreement with SEM/EDS data) and reduction of clay Fe(III). The large increase in the Fe(II) doublet content was consistent with the partial reduction of clay Fe(III), as noted in previous studies (Dong *et al.*, 2003a, 2003b; Komlos *et al.*, 2008). A small fraction of the Fe(II) doublet could be due to siderite (Table 2). A large pool of the Fe(II) became magnetically ordered at 4.5 K, based on a decrease in the Fe(II) doublet content with the concomitant presence of features that resembled abiotically and biotically reduced Garfield nontronite (Riberio *et al.*, 2009). In addition to the Fe(II) (paramagnetic and magnetically ordered species), sextet peaks due to residual Fe(III)-(oxyhydr)oxides (indicated by O, Figure 5f) were evident. Modeling of the 4.5 K spectrum was not attempted because of the following complexities:

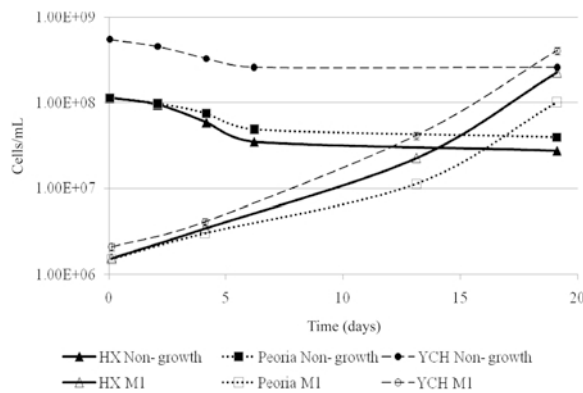

Figure 8. Colony-forming units (CFU) in the non-growth medium decreased slightly with time of bioreduction, while CFU in the M1 growth medium increased significantly. The error bars from duplicate tubes are shown or are smaller than the size of the symbols.

(1) precipitation of Fe(II) minerals such as siderite and vivianite (a high-energy peak of the spectrum was indicated by +) (Wade *et al.*, 1999); (2) partial reduction of clay-Fe(III) (Kukkadapu *et al.*, 2006); and (3) the presence of clay Fe(II) in different environments. Although a unique fit of the 4.5 K spectrum was not possible because of the complexities, the relative composition of various species and Mössbauer parameters are given in Table 5. The Fe(II) content increased at the expense of oxide-Fe(III) and phyllosilicate-Fe(III). Partial reduction of Fe (oxyhydr)oxides was further confirmed by SEM/EDS. The Fe (oxyhydr)oxides present in the untreated HX and Peoria samples were absent in the bioreduced samples (data not shown).

Bioreduction of Fe (oxyhydr)oxides and phyllosilicates resulted in the formation of certain new minerals (Table 4). Siderite XRD peaks emerged after bioreduction of the HX and YCH loess samples. The intensity of the 10 Å peak for the HX-loess sample in M1 medium with AQDS was significantly greater than the abiotic control and three other treatments (Figure 3a). The intensity of the 10 Å peak for the Peoria-loess sample in M1 treatments was greater than the abiotic control and non-growth treatments (Figure 3b). The 10 Å peak intensity for the YCH loess was greatest for the non-growth without AQDS treatment, however, and the peak intensities were equivalent for the other treatments (Figure 3c). The data collectively suggest that while the increased peak intensities for the 10 Å peak might be due to illite formation after bioreduction, other factors (such as sample preparation and K-fixation in smectite) might equally contribute to the observed intensity increases.

DISCUSSION

Microbial reduction of Fe(III)-containing minerals in loess sediments

Major Fe-containing minerals in soils and sediments, such as goethite, hematite, and smectite, can all serve as electron acceptors to support microbial growth. The results of the present study are, therefore, consistent with previous studies in showing that both Fe (oxyhydr)-oxides and phyllosilicates are important electron accep-

Table 4. Summary of reduced Fe minerals and biogenic products based on XRD and DRS analysis.

Reduced Minerals	Loess sediments		
	HX	Peoria	YCH
Goethite	x	x	x
Maghemite	?	–	x
Hematite	x	x	x
Smectite	x	x	x
Products:			
Siderite	x	–	x

https://doi.org/10.1346/CCMN.2010.0580409 Published online by Cambridge University Press

Table 5. Fit-derived Mössbauer parameters[1].

	<CS> (mm/s)	<Δ/ε> (mm/s)	st. dev. <Δ/ε> (mm/s)	<H>(T)	st. dev <H>(T)	% area
YCH						
RT						
Clay Fe(II)	1.142	2.637	0.171	——	——	41
Clay Fe(III)+(SP+SO)[2]	0.401	2.21	2.74	——	——	54
Hematite	0.424	−0.13	——	51.3	1	5
77 K						
Clay Fe(II)	1.258	2.866	0.341	——	——	38
Clay Fe(III)+(SP+SO)[2]	0.476	2.368	3.74	——	——	58
Hematite	0.505	−0.09	——	53.2	0.5	4
4.5 K						
Clay Fe(II)-1[3]	1.277	2.867	0.314	——	——	13
Clay Fe(II)-1[2]	1.16	2.946	1.441	——	——	25
Clay Fe(III)	0.509	0.805	0.485	——	——	42
PO Fe(III)[4]	0.239	0.32	——	24.9	3	10
Hematite[5]	0.334	0.04	——	52.6	2	10
YCH (AQDS + M1)						
RT						
Clay Fe(II)[6]	1.161	2.704	0.388	——	——	67
Clay Fe(III)[7]	0.378	0.863	0.466	——	——	33
77 K						
Clay Fe(II)[6]	1.281	2.909	0.371	——	——	64
Clay Fe(III)[7]	0.457	0.855	0.518	——	——	36

[1] <CS> – average center shift; <Δ> – average quadropole shift (only in the case of doublets); <ε> – average quadropole shift parameter (only in the case of sextets); <H> – average hyperfine field; st. dev. – standard deviation; area is ±2–3%
[2] SP = superparamagnetic; SO = substituted Fe-(oxyhydr)oxides (3 and 2 Gaussian components at RT and 77 K);
[3] Clay Fe(II)-1 – Fe-poor clay; clay Fe(II)-2 – Fe-rich clay
[4] PO = partially ordered Fe(III)-(oxyhydr)oxide
[5] Mostly hematite
[6] Combination peak due to clay Fe(II) and siderite/vivianite
[7] combination peaks due to clay Fe(III) and SO- and SP-(oxyhydr)oxides

tors to support microbial respiration (Zachara *et al.*, 1998; Favre *et al.*, 2002; Komlos *et al.*, 2007, 2008; Stucki *et al.*, 2007; Mohanty *et al.*, 2008; Anastácio *et al.*, 2008; Dong *et al.*, 2009). The DRS and aqueous geochemical data suggest that a fraction of certain minerals, such as goethite and hematite, were dissolved as a result of bioreduction even in the absence of AQDS (in non-growth medium), especially for the HX loess sample that had a large Fe(III) content. The dissolved goethite and hematite were insufficient to account for the total amount of Fe(II) measured by the Ferrozine and 1,10-phenanthroline methods, however, suggesting that phyllosilicate-Fe(III) was also bioreduced. The DRS and Mössbauer spectra of the YCH loess sample, which had the smallest Fe(III) content, revealed that only a fraction of goethite was bioreduced and most hematite remained. The results are consistent with the aqueous data which showed no significant difference in the Fe content between abiotic controls and bioreduced samples (Table 3). Thus, Ferrozine- and 1,10-phenanthroline-measured Fe(II) may have been largely derived from reduction of phyllosilicate-Fe(III). Indeed, Mössbauer data suggest reduction of phyllosilicate-Fe(III), probably from smectite. The Peoria loess Fe(III) content was intermediate and the DRS, XRD, and aqueous-ion concentration data do not suggest significant reduction of Fe(III) in goethite and hematite without AQDS. Most of the bioreduction measured by the Ferrozine and 1,10-phenanthroline (~20%) may, therefore, have been derived from the reduction of Fe(III) in phyllosilicates. These results confirm the prediction, based on the standard electrode potential, that the smectite structural Fe can be reduced prior to the Fe in oxides (Favre *et al.*, 2006).

The M1 growth medium significantly increased the Fe(III) bioreduction rate and extent in all three loess samples (Figures 6, 7), and the extent of bioreduction reached as high as 94% in the Peoria loess with AQDS. In the Peoria sample, an initially high Fe(II) content did not appear to inhibit the bioreduction. Because the Peoria sample had many Fe-containing minerals that included chlorite, illite, smectite, goethite, and hematite

https://doi.org/10.1346/CCMN.2010.0580409 Published online by Cambridge University Press

(Table 2), its nearly complete Fe(III) reduction suggests that Fe(III) in the phyllosilicates was also reduced. This bioreduction was coupled with cell growth (Figure 8), consistent with the study by Kostka *et al*. (2002). These results strongly indicate that under most favorable conditions, all Fe(III) in loess deposits is potentially available for microbial respiration.

In summary, the results of this study suggest that Fe(III) in Fe (oxyhydr)oxides and phyllosilicates, commonly found in loess deposits, is an important source of electron acceptors. Growth medium (M1) and electron shuttling compounds such as AQDS greatly enhanced the rate and extent of Fe(III) bioreduction.

Mineralogical transformations as a result of bioreduction

Siderite was detected in the bioreduced materials using XRD. The presence of siderite, coupled with aqueous-chemistry data, suggests partial dissolution of Fe (oxyhydr)oxides and phyllosilicates, consistent with previous results (Dong *et al.*, 2003b). A previous study suggested a biogenic origin for calcite nano-fibers during pedogenesis of loess samples (Xu and Chen, 2008) and proposed that organic compounds derived from microbial activities controlled the formation of the calcite nano-fibers. Li *et al.* (2004) used sulfate-reducing bacteria to reduce structural Fe(III) in nontronite and observed biogenic calcite, although Fe(II) was abundant and siderite was expected. The authors speculated that Fe(II) might have been removed by precipitation of pyrite. In the present experiments, siderite precipitated because no sulfide was available to form pyrite. In this case, siderite, rather than calcite, formed. Regardless of specific minerals, the observation of siderite supported a possible biogenic origin of carbonate minerals in loess deposits, possibly formed during pedogenesis (Xu and Chen, 2008).

Implications for bioreduction and geochemical transformations of Fe(III) in loess deposits

Mutual interactions between bacteria and loess sediments have important implications for both bacteria and loess sediments. Loess deposits contain minerals to sustain microbial activity which in turn can influence the physical and chemical properties of loess sediments. The present study has shown that, under the most favorable conditions (*i.e.* aqueous environment with Fe-reducing bacteria and carbon substrates), loess deposits can actually support microbial respiration and growth. These special conditions can typically occur for natural loess deposits with storm events or with agricultural use of loess soils. Loess deposits contain organic carbon and nitrogen (0.06–0.13% and ~0.04%) as well as many trace elements (such as Al, Si, Na, Ca, Mg, K, Fe, Be, Pb, Mn, Ga, Cr, Ni, Ti, Cu, V, Zr, B, Co, Ba, Sr, Sc, Ag, Sb, and Y) (Chinese Academy of Sciences, 1979; Xu, 1993). The relative amounts of these elements vary depending on the sources and formation process of loess deposits. Loess also contains other nutrients, such as phosphorous and amino acids (Curry *et al.*, 1994). As long as water is available, loess deposits are, therefore, capable of sustaining microbial respiration. One important type of respiration may be *via* Fe reduction because Fe(III)-containing minerals are abundant and anaerobic environments can occur in loess sediments. Indeed, many Fe(III)-reducing bacteria have been isolated from clay-rich sedimentary deposits (Zavarzina *et al.*, 2003; Shelobolina *et al.*, 2005, 2007). Native Fe-reducing micro-organisms in certain loess deposits should be desiccation tolerant, as water is scarce in such environments. Indeed, radiation- and desiccation-resistant *Deinococcus radiodurans* has been shown to be capable of reducing solid-phase Fe(III) in the presence of electron shuttles (Fredrickson *et al.*, 2000).

In many parts of the world, loess soils are used extensively for agriculture (Smalley, 1975; Smalley *et al.*, 2001). Under these conditions, many Fe-reducing micro-organisms may potentially become active in reducing structural Fe(III) of Fe (oxyhydr)oxides and phyllosilicates, thus altering the physical and chemical properties of clay minerals and loess soils (Stucki *et al.*, 2006). Under these circumstances, micro-organisms may significantly impact soil fertility and contaminant mobility/retention through bioreduction of structural Fe(III) in clays and clay minerals.

CONCLUSIONS

The Fe(III) in Fe (oxyhydr)oxides and phyllosilicates common in loess deposits are bioreducible. A growth medium (M1) and the availability of electron shuttling compounds, such as anthraquinone-2, 6-disulfonate, significantly enhanced the rate and extent of bioreduction of Fe(III) in Fe mineral phases. As a result of microbial reduction, siderite formed. These results suggest that Fe(III) in the various loess deposit minerals is potentially an important electron acceptor to support respiration of Fe-reducing bacteria. These results have important implications for understanding the interactions between micro-organisms and clays in fine-grained loess deposits.

ACKNOWLEDGMENTS

Dr Jason Rech and Huifan Xu donated the loess samples for study. This research was supported in part by student grants to MEB from Miami University (Undergraduate Research Grant, 2007). MEB is grateful to Dr Richard Edelmann and Matt Dulley for their help with SEM/EDS training. The authors thank Dr John P. Morton for his help with the DCP analyses and XRD training, and Dr John Rakovan for his help with the XRD analyses. The work was supported by grants from the U.S. Department of Energy (DE FG02-07ER64369) and the National Science Foundation (EAR-0345307) to HD. A portion of the research was performed using EMSL, a national scientific

user facility sponsored by the Department of Energy's Office of Biological and Environmental Research located at Pacific Northwest National Laboratory. Two anonymous reviewers and the associate editor, Dr William F. Jaynes, are acknowledged for their constructive comments which greatly improved the quality of this manuscript.

REFERENCES

Amonette, J.E. and Templeton, C. (1998) Improvements to the quantitative assay of nonrefractory minerals for Fe(II) and total Fe using 1, 10-Phenanthroline. *Clays and Clay Minerals*, **46**, 51–62.

Anastácio, A.S., Aouad, A., Sellin, P., Fabris, J.D., Bergaya, F., and Stucki, J.W. (2008) Characterization of a redox-modified clay mineral with respect to its suitability as a barrier in radioactive waste confinement. *Applied Clay Science*, **39**, 172–179.

Andrade, S., Hypolito, R., Ulbrich, H.H., and Silva, M.L. (2002) Technical note on iron (II) oxide determination in rocks and minerals. *Chemical Geology*, **182**, 85–89

Balsam, W.L. and Ji, J.F. (1999) Mineralogic variations in the Chinese loess sequence determined by NUV/VIS/NIR reflectance spectra. *GSA Abstracts with Programs*, **31**, A-54.

Bazylinski, D.A. and Frankel, R.B. (2004) Magnetosome formation in prokaryotes. *Nature Review Microbiology*, **2**, 217–230.

Chanal, A., Chapon, V., Benzerara, K., Barakat, M., Christen, R., Achouak, W., Barras, F., and Heulin, T. (2006) The desert of Tataouine: an extreme environment that hosts a wide diversity of microorganisms and radiotolerant bacteria. *Environmental Microbiology*, **8**, 514–525.

Chen, T.H., Xu, H.F., Ji, J.F., Chen, J., and Chen, Y. (2003) Formation mechanism of ferromagnetic minerals in loess of China: TEM investigation. *Chinese Science Bulletin*, **48**, 2259–2266.

Chen, T., Xu, H., Xie, Q., Chen, J., Ji, J., and Lu, H. (2005) Characteristics and genesis of maghemite in Chinese loess and paleosols: Mechanism for magnetic susceptibility enhancement in paleosols. *Earth and Planetary Science Letters*, **240**, 790–802.

Chinese Academy of Sciences (1979) *Comprehensive Survey of Qinghai Lake*. Science Publishing House, Beijing, China (in Chinese).

Curry, G.B., Theng, B.K.G., and Zheng, H.H. (1994) Amino acid distribution in a loess-paleosol sequence near Luochuan, Loess Playeau, China. *Organic Geochemistry*, **22**, 287–298.

Dolgoff, A. (1998) *Physical Geology*, updated version. Houghton Mifflin Company, Boston, Massachussets, USA, pp. 499–504.

Dong, H., Kukkadapu, R.K., Fredrickson, J.K., Zachara, J.M., Kennedy, D.W., and Kostandarithes, H.M. (2003a) Microbial reduction of structural Fe(III) in illite and goethite. *Environmental Science & Technology*, **37**, 1268–1276.

Dong, H., Kostka, J.E. and Kim, J. (2003b) Microscopic evidence for microbial dissolution of smectite. *Clays and Clay Minerals*, **51**, 502–512.

Dong, H., Jaisi, D.P., Kim, J.W., and Zhang, G. (2009) Microbe-clay mineral interactions: a Review. *American Mineralogist*, **94**, 1505–1519.

Dorn, R.I. and Oberlander, T.M. (1981) Microbial origin of desert varnish. *Science*, **213**, 1245–1247.

Favre, F., Tessier, D., Abdelmoula, M., Genin, J.M., Gates, W.P., and Boivin, P. (2002) Iron reduction and changes in cation exchange capacity in intermittently waterlogged soil. *European Journal of Soil Science*, **53**, 175–183.

Favre, F., Stucki, J.W., and Boivin, P. (2006) Redox properties of structural Fe in ferruginous smectite. A discussion of the standard potential and its environmental implications. *Clays and Clay Minerals*, **54**, 466–472.

Fredrickson, J.K., Kostandarithes, H.M., Li, S.W., Plymale, A.E., and Daly, M.J. (2000) Reduction of Fe(III), Cr(VI), U(VI), and Tc(VII) by *Deinococcus radiodurans* R1. *Applied and Environmental Microbiology*, **66**, 2006–2011.

Gallet, S., Jahn, B.M., and Torii, M. (1996) Geochemical characterization of the Luochuan loess-paleosol sequence, China, and paleoclimatic implications. *Chemical Geology*, **133**, 67–88.

Gates, W.P., Jaunet, A., Tessier, D., Cole, M.A., Wilkinson, H.T., and Stucki, J.W. (1998) Swelling and texture of iron bearing smectites reduced by bacteria. *Clays and Clay Minerals*, **46**, 487–497.

Grimley, D.A., Follmer, L.R., and McKay, E.D. (1998) Magnetic susceptibility and mineral zonations controlled by provenance in loess along the Illinois and central Mississippi River valleys. *Quaternary Research*, **49**, 24–36.

Grimley, D.A. (2000) Glacial and nonglacial sediment contributions to Wisconsin Episode loess in the central United States. *Geological Society of America Bulletin*, **112**, 1475–1495.

Hu, X.F., Lu, H., Xu, Q., Dong, L.J., and Hu, X. (2004) Red ratings for loess-paleosol sequences on China's loess plateau and their paleo-climatic implications. *Pedosphere* **14**, 430–440.

Jahn, B.M., Gallet, S., and Han, J.M. (2001) Geochemistry of the Xining, Xifeng and Jixian sections, China: Eolian dust provenance and paleosol evolution during the last 140 ka. *Chemical Geology*, **178**, 71–94.

Jaisi, D.P., Kukkadapu, R.K., Eberl, D.D., and Dong, H. (2005) Control of Fe(III) site occupancy on the rate and extent of microbial reduction of Fe(III) in nontronite. *Geochimica et Cosmochimica Acta*, **69**, 5429–5440.

Jaisi, D.P., Dong, H., and Liu, C.X. (2007) Influence of biogenic Fe(II) on the extent of microbial reduction of Fe(III) in clay minerals nontronite, illite, and chlorite. *Geochimica et Cosmochimica Acta*, **71**, 1145–1158

Ji, J.F., Balsam, W.L., Chen, J., and Liu, L.W. (2002) Rapid and precise measurement of hematite and goethite concentrations in the Chinese loess sequences by diffuse reflectance spectroscopy. *Clays and Clay Minerals*, **50**, 210–218.

Ji, J., Chen, J., Jin, L., Zhang, W., Balsam, W., and Lu, H. (2004) Relating magnetic susceptibility (MS) to the simulated thematic mapper (TM)bands of the Chinese loess: Application of TM image for soil MS mapping on Loess Plateau. *Journal of Geophysical Research*, **109**, B05102.

Jia, R.F., Yan, B.Z., Li, R.S., Fan, G.C., and Lin, B.H. (1996) Characteristics of magnetotactic bacteria in Duanjiapo loess section, Shaanxi province and their environmental significance. *Science in China Series D – Earth Sciences*, **39**, 478–485.

Judd, D.B. and Wyszecki, G. (1975) *Color in Business, Science, and Industry*. John Wiley & Sons, New York, 553 pp.

Kim, J.W., Dong, H., Seabaugh, J., Newell, S.W., and Eberl, D.D. (2004) Role of microbes in the smectite-to-illite reaction. *Science*, **303**, 830–832.

Komlos, J., Kukkadapu, R.K., Zachara, J.M., and Jaffe, P.R. (2007) Biostimulation of iron reduction and subsequent oxidation of sediment containing Fe-silicates and Fe-oxides: Effect of redox cycling on Fe(III) bioreduction. *Water Research*, **41**, 2996–3004.

Komlos, J., Peacock, A., Kukkadapu, R.K., and Jaffe, P.R. (2008) Long-term dynamics of uranium reduction/reoxidation under low sulfate conditions. *Geochimica et Cosmochimica Acta*, **72**, 3603–3615.

Kostka, J.E., Haefele, E., Viehweger, R., and Stucki J.W.

(1999a) Respiration and dissolution of Fe(III)-containing clay minerals by bacteria. *Environmental Science & Technology*, **33**, 3127–3133.

Kostka, J.E., Wu, J., Nealson, K.H., and Stucki, J.W. (1999b) The impact of structural Fe(III) reduction by bacteria on the surface chemistry of clay minerals. *Geochimica et Cosmochimica Acta*, **63**, 3705–3713.

Kostka, J.E., Dalton, D.D., Skelton, H., Dollhopf, S., and Stucki, J.W. (2002) Growth of iron(III)-reducing bacteria on clay minerals as the sole electron acceptor and comparison of growth yields on a variety of oxidized iron forms. *Applied and Environmental Microbiology*, **68**, 6256–6262.

Kukkadapu, R.K., Zachara, J.M., Fredrickson, J.K., and Kennedy, D.W. (2004) Biotransformation of two-line silica-ferrihydrite by a dissimilatory Fe(III)-reducing bacterium: formation of carbonate green rust in the presence of phosphate. *Geochimica et Cosmochimica Acta*, **68**, 2799–2814.

Kukkadapu, R.K., Zachara, J.M., Fredrickson, J.K., McKinley, J.P., Kennedy, D.W., Smith, S.C., and Dong, H.L. (2006) Reductive biotransformation of Fe in shale-limestone saporite containing Fe(III) oxides and Fe(II)/Fe(III) phyllosilicates. *Geochimica et Cosmochimica Acta*, **70**, 3662–3676.

Leigh, D.S. (1994) Roxana silt of the Upper Mississippi Valley – lithology, source, and paleoenvironment. *Geological Society of America Bulletin*, **106**, 430–442.

Li, Y.L., Zhang, C.L., Yang, J., Deng, B., and Vali, H. (2004) Dissolution of nontronite NAu-2 by a sulfate-reducing bacterium. *Geochimica et Cosmochimica Acta*, **68**, 3251–3260.

Lovley, D.R. (1991) Dissimilatory Fe(lll) and Mn(lV) reduction. *Microbiology Review*, **55**, 259–287.

Maat, P.B. and Johnson, W.C. (1996) Thermoluminescence and new 14C age estimates for late Quaternary loesses in southwestern Nebraska. *Geomorphology*, **17**, 115–128.

Mohanty, S.R., Kollah, B., Hedrick, D.B., Peacock, A.D., Kukkadapu, R.K., and Roden, E.E. (2008) Biogeochemical processes in ethanol stimulated uranium contaminated subsurface sediments. *Environmental Science & Technology*, **42**, 4384–4390.

Moore, D.M. and Reynolds Jr., R.C. (1997) *X-ray Diffraction and the Identification and Analysis of Clay Minerals.* Oxford University Press, New York.

Muhs, D.R. and Bettis III, E.A. (2000) Geochemical variations in Peoria Loess of western Iowa indicate paleowinds of midcontinental North America during the last glaciation. *Quaternary Research*, **53**, 49–61.

Muhs, D.R. and Zárate, M. (2001) Eolian records of the Americas and their paleoclimatic significance. Pp. 183–216 in: *Interhemispheric Climate Linkages* (V. Markgraf, editor). Academic Press, San Diego.

Myers, C.R. and Nealson, K.H. (1988) Bacterial manganese reduction and growth with manganese oxide as the sole electron acceptor. *Science*, **240**, 1319–1321

Osman, S., Peeters, Z., La Duc, M.T., Mancinelli, R., Ehrenfreund, P., and Venkateswaran, K. (2008) Effect of shadowing on survival of bacteria under conditions simulating the Martian atmosphere and UV radiation. *Applied and Environmental Microbiology*, **74**, 959–970.

Perry, R.S., Engel, M.H., Botta, O., and Staley, J.T. (2003) Amino acid analyses of desert varnish from the Sonoran and Mojave Deserts. *Geomicrobiology Journal*, **20**, 427–438.

Rancourt, D.G. and Ping, J.Y. (1991) Voigt-based methods for arbitrary-shape static hyperfine parameter distributions in Mössbauer spectroscopy. *Nuclear Instrument Methods in Physics research*, Sec. B., **58**, 85–97.

Riberio, F.R., Fabris, J.D., Kostka, J.E., Komadel, P., and Stucki, J.W. (2009) Comparisons of structural iron reduction in smectites by bacteria and dithionite: II. A variable-temperature Mössbauer spectroscopic study of Garfield nontronite. *Pure and Applied Chemistry*, **81**, 1499–1509.

Roberts, H.M., Muhs, D.R., Wintle, A.G., Duller, G.A.T., and Bettis, III, E. (2003) Unprecedented last-glacial mass accumulation rates determined by luminescence dating of loess from western Nebraska. *Quaternary Research*, **59**, 411–419.

Shelobolina, E.S., Vanpraagh, C.G., and Lovley, D.R. (2003) Use of ferric and ferrous iron containing minerals for respiration by *Desulfitobacterium frappieri*. *Geomicrobiology Journal*, **20**, 143–156.

Shelobolina, E.S., Pickering, S.M., and Lovley, D.R. (2005) Fe-cycle bacteria from industrial clays mined in Georgia, USA. *Clays and Clay Minerals*, **53**, 580–586.

Shelobolina, E.E., Nevin, K.P., Blakeney-Hayward, J.D., Johnsen, C.V., Plaia, T.W., Krader, P., Woodard, T., Holmes, D.E., VanPraagh, C.G., and Lovley, D.R. (2007) Geobacter pickeringii sp nov., Geobacter argillaceus sp nov., and Pelosinus fermentans gen. nov., sp nov., isolated from subsurface kaolin lenses. *International Journal of Systematic and Evolutionary Microbiology*, **57**, 126–135.

Smalley, I.J. (1975) *Lithology and Genesis*. Dowden, Hutchinson, and Ross, New York, 429 p.

Smalley, I.J., Jefferson, I.F., Dijkstra, T.A., and Derbyshire, E. (2001) Some major events in the development of the scientific study of loess. *Earth-Science Reviews* **54**, 5–18.

Stookey, L.L. (1970) Ferrozine – a new spectrophotometric reagent for iron. *Analytical Chemistry*, **42**, 779–781.

Stucki, J.W. (2006) Properties and behavior of iron in clay minerals. Pp. 423–476 in: *Handbook of Clay Science* (F. Bergaya, G. Lagaly, and B.G.K. Theng, editors). Elsevier, Amsterdam.

Stucki, J.W. and Kostka, J.E. (2006) Microbial reduction of iron in smectite. *Comptes Rendus Geoscience*, **338**, 468–475.

Stucki, J.W., Lee, K., Zhang, L., and Larson, R.A. (2002) The effects of iron oxidation state on the surface and structural properties of smectites. *Pure and Applied Chemistry*, **74**, 2079–2092.

Stucki, J.W., Lee, K., Goodman, B.A., and Kostka, J.E. (2007) Effects of in situ biostimulation on iron mineral speciation in a sub-surface soil. *Geochimica et Cosmochimica Acta*, **71**, 835–843.

Sun, J.M. (2002) Source Regions and formation of the loess sediments on the high mountain regions of northwest China. *Quaternary Research*, **3**, 341–351.

Thorp, J. and Smith, H.T.U. (1952) *Pleistocene eolian deposits of the United States, Alaska, and parts of Canada. National Research Council Committee for the Study of Eolian Deposits*. Geological Society of America, New York.

Van Der Zee, C., Slomp, C.P., Rancourt, D.G., de Lange, G.J., and Raaphorst, W.V. (2005) A Mössbauer spectroscopic study of the iron redox transition in eastern Mediterranean sediments. *Geochimica et Cosmochimica Acta*, **69**, 441–453.

Wade, L., Agresti, D.G., Wdowiak, T.J., and Armendarez, L.P. (1999) A Mössbauer investigation of iron-rich terrestrial hydrothermal vent systems: lessons for Mars exploration. *Journal of Geophysical Research*, **104**, 8489–8507.

Wang, F., Wang, P., Chen, M., and Xiao, X., (2004) Isolation of extremophiles with the detection and retrieval of Shewanella strains in deep-sea sediments from the west Pacific. *Extremophiles*, **8**, 165–168.

Wang, H., Follmer, L.R., and Liu, J.C. (2000) Isotope evidence of El Niño – southern oscillation cycles in loess-paleosol record in the central United States. *Geology*, **28**, 771–774.

Wang, H., Hughes, R., Steele, J.D., Lepley, S.W., and Tian, J. (2003) Correlation of climate cycles in middle Mississippi

Valley loess and Greenland ice. *Geology*, **31**, 179–182.
Xu, H.F. and Chen, T. (2008) Microbe-templated calcite nanofibers in Chinese Loess Plateau: Potential carbon dioxide sinker. *Geochimica et Cosmochimica Acta*, **72**, A1046.
Xu, Y. (1993) *Clay Mineralogy in Salt Lakes of China*. 208 pp. Science Publishing House, Beijing (in Chinese).
Zachara, J.M., Fredrickson, J.K., Li, S.M., Kennedy, D.W., Smith, S.C., and Gassman, P.L. (1998) Bacterial reduction of crystalline Fe(III) oxides in single phase suspensions and subsurface materials. *American Mineralogist*, **83**, 1426–1443.
Zavarzina, D.G., Alekseev, A.O., and Alekseeva, T.V. (2003) The role of iron-reducing bacteria in the formation of magnetic properties of steppe soils. *Eurasian Soil Science*, **36**, 1085–1094.

(*Received 8 August 2009; revised 23 June 2010; Ms. 346; A.E. W.F. Jaynes*)